

## Electronic Supplementary Information

### **Hollow transition metal hydroxide octahedral microcages for single particle surface-enhanced Raman spectroscopy**

Mansha Gao,<sup>‡a</sup> Peng Miao,<sup>‡a</sup> Xijiang Han,<sup>\*a</sup> Cheng Sun,<sup>a</sup> Yan Ma,<sup>a</sup> Yali Gao,<sup>a</sup> and Ping Xu<sup>\*a</sup>

<sup>a</sup>. MIIT Key Laboratory of Critical Materials Technology for New Energy Conversion and Storage, School of Chemistry and Chemical Engineering, Harbin Institute of Technology, Harbin 150001, China.

Email: p xu@hit.edu.cn; hanxijiang@hit.edu.cn

<sup>‡</sup>These authors contributed equally.

## Supplementary Figures and Tables

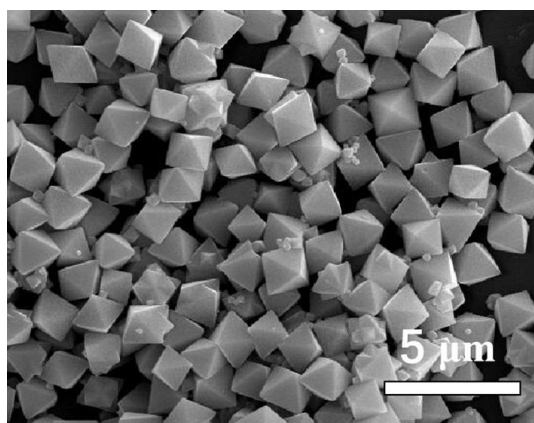


Fig. S1 SEM image of as-prepared precursor  $\text{Cu}_2\text{O}$  octahedron ( $1.5 \mu\text{m}$ ).

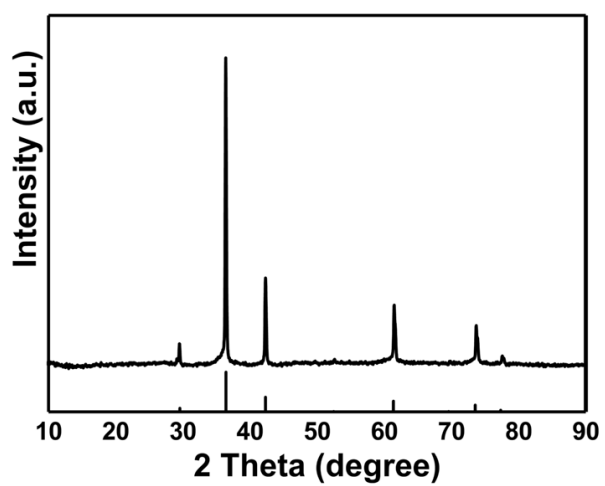
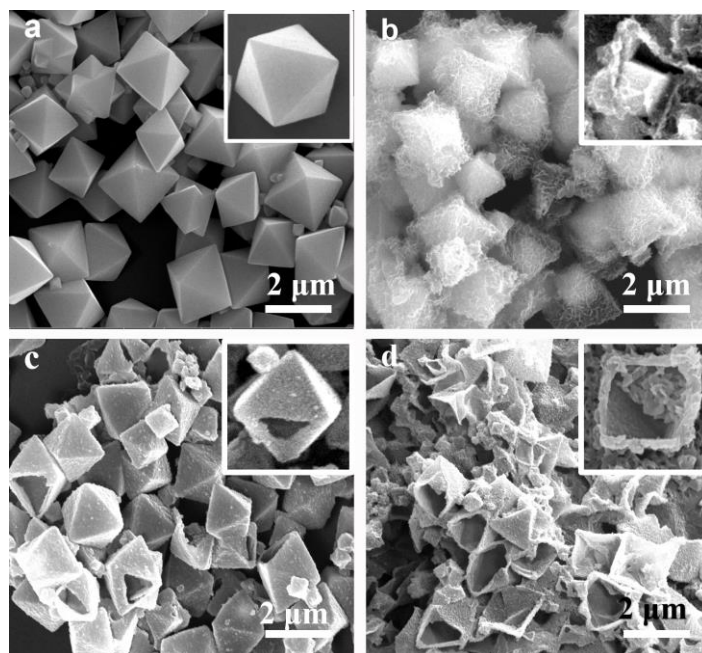
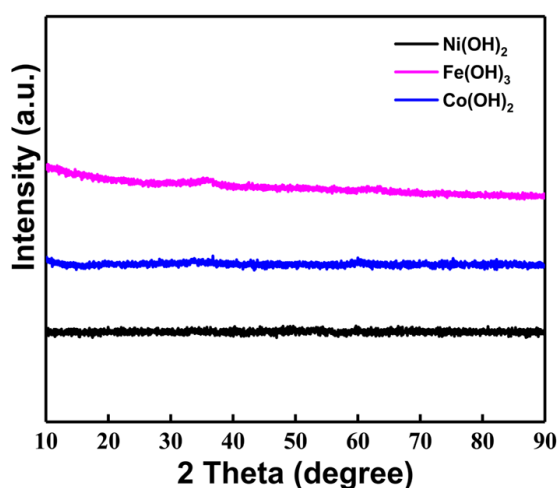


Fig. S2 XRD pattern of as-prepared precursor  $\text{Cu}_2\text{O}$  octahedron ( $1.5 \mu\text{m}$ ).



**Fig. S3** SEM images collected at different reaction times: (a) 0 min, (b) 3 min, (c) 6 min, (d) 9 min. It can be clearly observed that the precipitation of transition metal hydroxide is synchronized with the dissolution of  $\text{Cu}_2\text{O}$  from a gappy particle (inset in b). As the reaction proceeds,  $\text{Cu}_2\text{O}$  core gradually disappears and the stacking of hydroxide nanosheets is gradually dense. The whole system is transformed from solid to hollow structure. When the reaction exceeds the optimal time of 9 min, the disappearance of template breaks the balance of the collaborative etching process, and the growth of hydroxides becomes scattered (inset in d).



**Fig. S4** XRD pattern of hollow  $\text{M(OH)}_x$  ( $\text{M}=\text{Fe}, \text{Co}, \text{Ni}$ ) octahedral microcages ( $1.5 \mu\text{m}$ ) with  $\text{Cu}_2\text{O}$  as sacrificial templates.

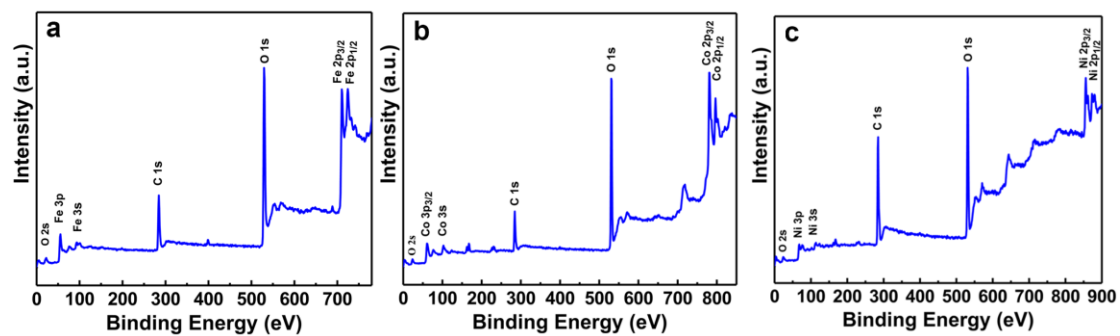


**Fig. S5** Full range XPS spectra of the as-prepared (a) Fe(OH)<sub>3</sub>, (b) Co(OH)<sub>2</sub>, and (c) Ni(OH)<sub>2</sub>.

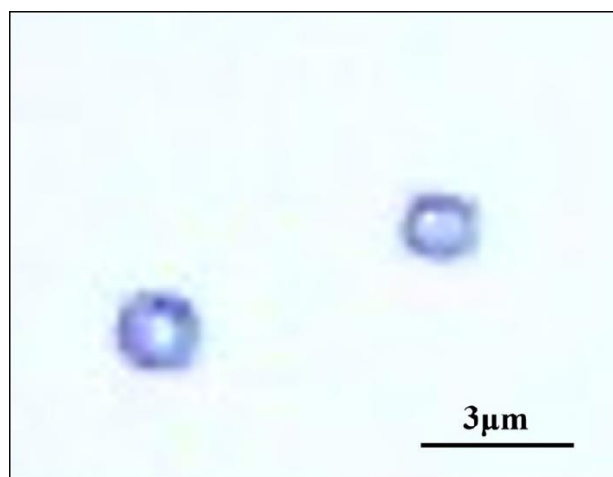


**Fig. S6** Optical image of monodispersed M(OH)<sub>x</sub> micron-octahedron under Renishaw confocal Raman microscope.

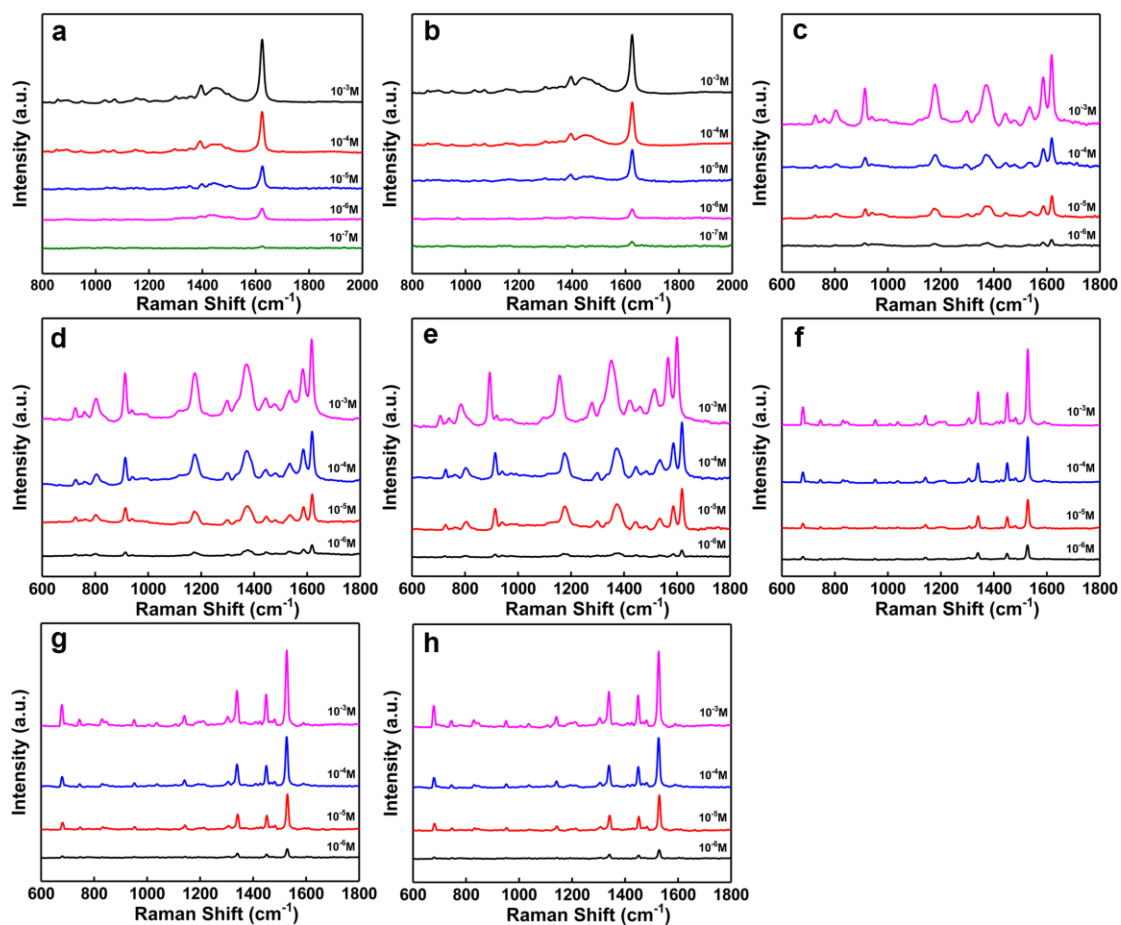


**Fig. S7** Concentration-dependent SERS spectra of MB (b-c), CV (d-f) and CuPc (g-i) on  $\text{Fe}(\text{OH})_3$  (a, c and f),  $\text{Co}(\text{OH})_2$  (b, d and g), and  $\text{Ni}(\text{OH})_2$  (e and h) substrates under 532 nm laser excitation ( $148\mu\text{w}$ ).

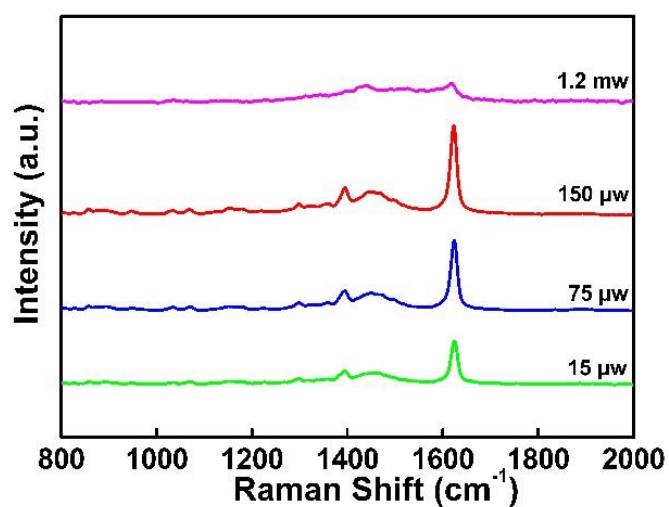


**Fig. S8** Raman spectra of MB ( $10^{-5}$  M) molecules on  $\text{Ni}(\text{OH})_2$  substrates under different laser powers.

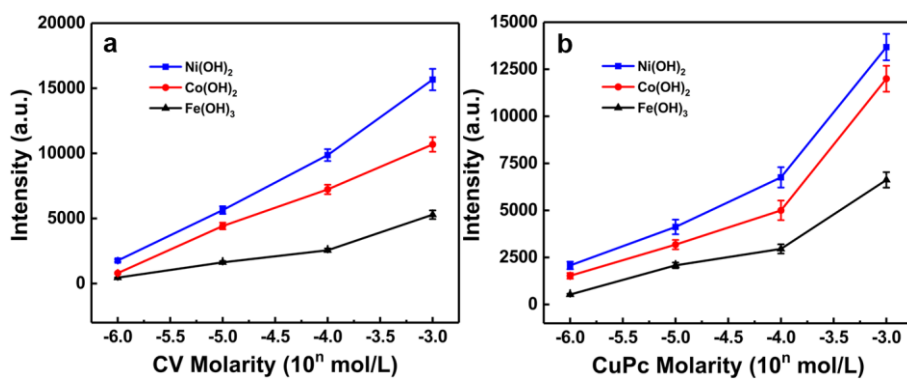


**Fig. S9** (a) The Raman intensity of CV at  $1618\text{ cm}^{-1}$  as a function of the molecular concentration on the  $M(\text{OH})_x$  substrate, (b) The Raman intensity of CuPc at  $1528\text{ cm}^{-1}$  as a function of the molecular concentration on the  $M(\text{OH})_x$  substrate.

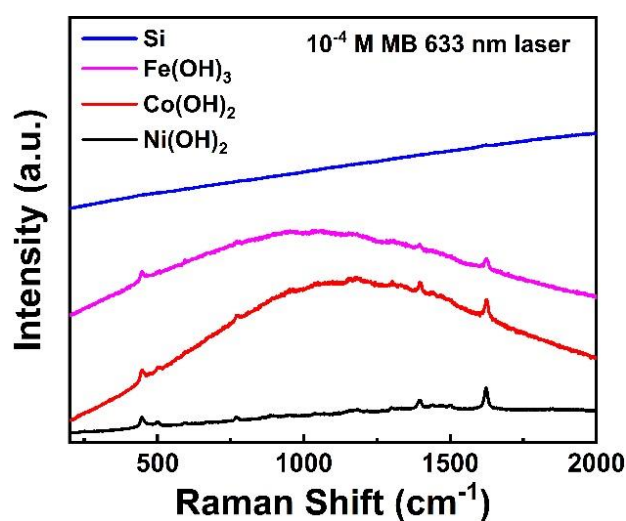


**Fig. S10** Raman spectra of MB ( $10^{-4}$  M) molecules on three substrates collected with 633 nm laser.

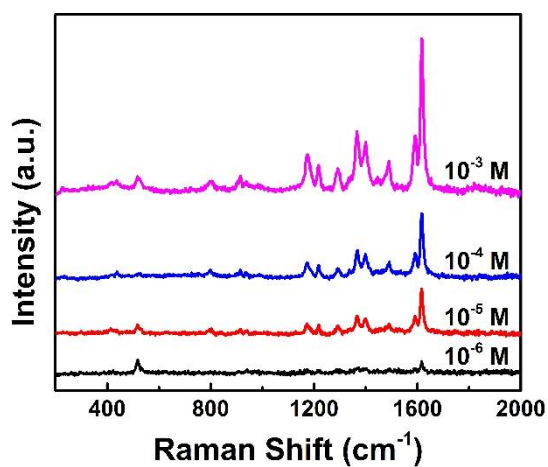


**Fig. S11** Concentration-dependent SERS spectra of malachite green dye on the  $\text{Ni}(\text{OH})_2$  substrate collected with 532 nm laser.

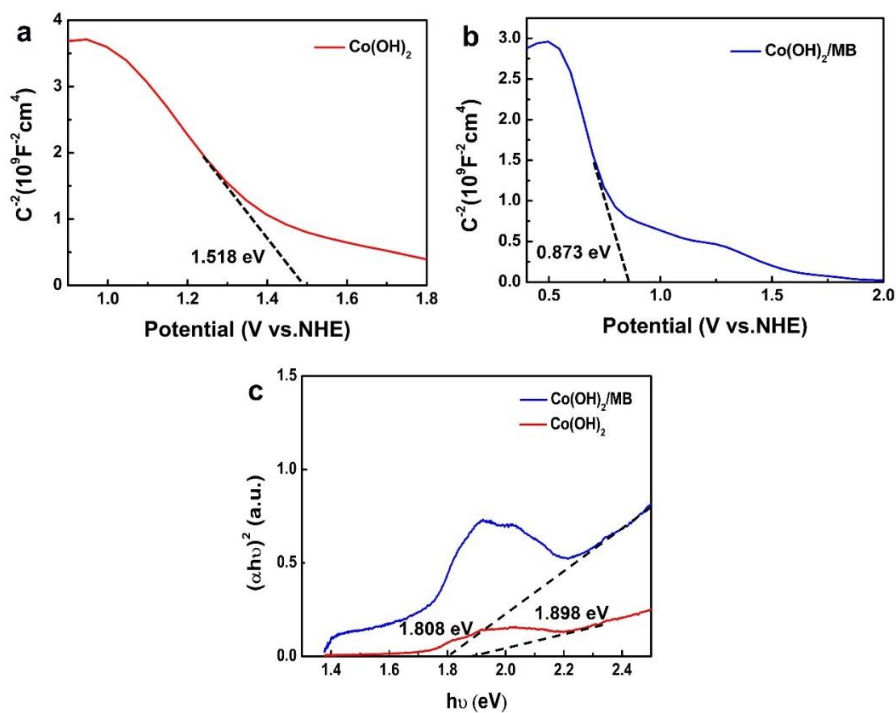


**Fig. S12** Electrochemical Mott–Schottky (M–S) plots of  $\text{Co(OH)}_2$  (a) and  $\text{Co(OH)}_2/\text{MB}$  (b). (c) Tauc plot of  $\text{Co(OH)}_2$  before and after MB adsorption.

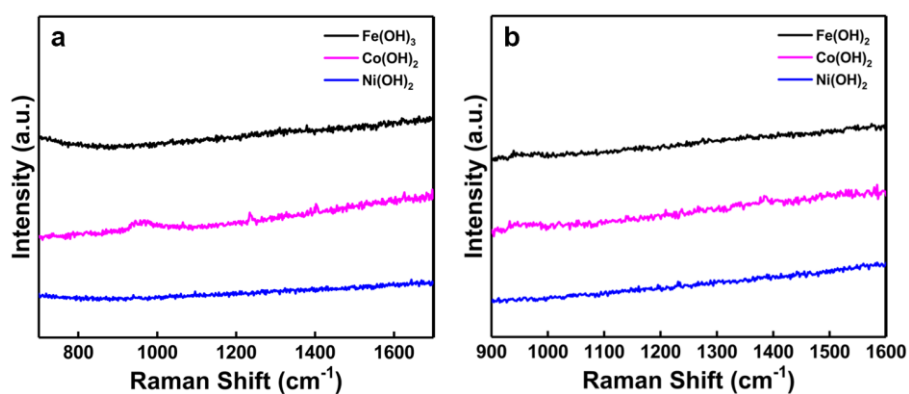


**Fig. S13** SERS spectra of pyrene (a) and benzopyrene (b) on  $\text{M(OH)}_x$  ( $\text{M}=\text{Fe}, \text{Co}, \text{Ni}$ ) substrates at 532 nm laser excitation.

**Table S1.** Enhancement factor of some SERS-active metal hydroxides and metal oxides based on charge transfer mechanism.

Material(s)	Morphology	Probes	EF	Ref.
TiO <sub>2</sub>	10 nm particle	4-MBA	10 <sup>3</sup>	1
ZnO	nanocage	4-MBA	10 <sup>5</sup>	2
Fe <sub>2</sub> O <sub>3</sub>	sphere	4-MBY	10 <sup>4</sup>	3
CuO	nanocrystals	4-MBY	10 <sup>2</sup>	4
W <sub>18</sub> O <sub>49</sub>	nanowire	R6G	10 <sup>5</sup>	5
Co(OH) <sub>2</sub>	nanosheet	DTTCI	10 <sup>3</sup>	6
Ni(OH) <sub>2</sub>	Hollow octahedra	MB	10 <sup>3</sup>	This work

**Table S2.** Deviation of binding energy after adsorption of MB molecule on different transition metal hydroxides substrate

Sample	N 1 s binding energy (eV)	
	Peak I	Peak II
Fe(OH) <sub>3</sub> /MB	399.7	400.7
Co(OH) <sub>2</sub> /MB	399.8	400.8
Ni(OH) <sub>2</sub> /MB	399.7	401.9



**Table S3.** The Binding Energy of metal ions before and after adsorption of MB molecule

Metal ion	Fe <sup>3+</sup>		Co <sup>2+</sup>		Ni <sup>2+</sup>	
Orbital split	2P <sub>1/2</sub>	2P <sub>3/2</sub>	2P <sub>1/2</sub>	2P <sub>3/2</sub>	2P <sub>1/2</sub>	2P <sub>3/2</sub>
Binding energy before absorbing MB (eV)	724.6 eV	711.0 eV	796.8 eV	781.0 eV	873.7 eV	855.7 eV
Binding energy after absorbing MB (eV)	725.2 eV	711.6 eV	797.4 eV	781.6 eV	874.2 eV	856.2 eV
The shift amount of binding energy $\Delta$ (eV)	0.6 eV		0.6 eV		0.5 eV	

## Calculation of enhancement factor.

The enhancement factor was calculated according to the following equation (Angew. Chem. Int. Ed. 2017, 56, 9851 – 9855):

$$EF = (I_{SERS} / N_{SERS}) / (I_{NR} / N_{NR})$$

where  $I_{SERS}$  and  $I_{NR}$  are the Raman intensities of MB molecule on  $M(OH)_x$  substrate and that without substrate (Si substrate in this study).  $N_{SERS}$  is the number of molecules adsorbed on the  $M(OH)_x$  substrate within the laser spot area, and  $N_{NR}$  stands for the number of molecules excited on the Si substrate. In order to obtain the value of  $N_{NR}$ , 100  $\mu\text{L}$  of MB solution (1 mM) was dropped onto the Si wafer ( $0.5 \times 0.5 \text{ cm}^2$ ).  $N_{NR}$  can be estimated by the following equation:

$$N_{NR} = c_{NR} V (A_{\text{beam}}/A) N_A$$

where  $A_{\text{beam}} = \pi(d/2)^2$  is the area of the focal spot of the laser,  $d$  is the diameter of the light spot estimated by  $d = 1.22 \lambda/\text{NA}$ ,  $\lambda$  is the incident laser wavelength, i.e., 532 nm, and the numerical aperture (NA) of the objective lens  $\text{NA} = 0.75$ . Thereby, laser spot size is approximately  $1.87 \mu\text{m}^2$ .  $A$  is the area of MB molecule layer which equal to the area of Si wafer ( $0.25 \text{ cm}^2$ ).  $N_A$  stands for Avogadro's constant. Therefore,  $N_{NR}$  equals to:

$$N_{NR} = 40 \mu\text{L} \times 0.001 \text{ mol} / \text{L} \times 0.59 \mu\text{m}^2 / 0.25 \text{ cm}^2 \times 6.02 \times 10^{23} \text{ mol}^{-1} = 5.68 \times 10^8$$

Moreover,  $N_{SERS}$  is the number of adsorbed molecules scattered in the area of laser beam, which can be estimated by the following equation:

$$N_{SERS} = A_{\text{beam}}/\sigma$$

where  $\sigma$  is the area occupied by a molecule of adsorbent at monolayer coverage, which is estimated to  $\sim 0.5 \text{ nm}^2$ . It should be mentioned that the surface coverage must remain smaller than one monolayer when using this equation. The concentration of the MB solution was controlled lower than  $1 \times 10^{-4} \text{ M}$  to prevent the supersaturation adsorption of probe molecule onto  $M(OH)_x$  substrate.  $N_{SERS}$  is calculated to be  $1.18 \times 10^6$ . The intensity at  $1626 \text{ cm}^{-1}$  of MB molecule on Si and the intensity at  $1624 \text{ cm}^{-1}$  on  $\text{Ni(OH)}_2$  substrate were used to calculate EF values. Here  $I_{SERS} = 27000$ , and  $I_{NR} = 5530$  (Fig. S14). By substituting these values into the equation, EF is calculated to be  $2.35 \times 10^3$ .

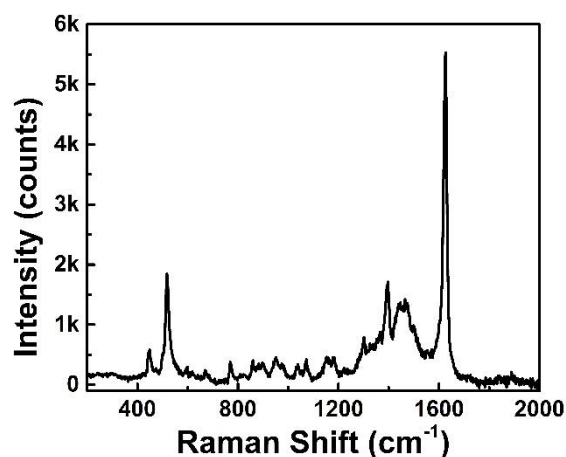


**Fig. S14** The normal Raman spectrum of pure MB (1 mM) on Si substrate.

## References:

1. L. B. Yang, X. Jiang, W. D. Ruan, B. Zhao, W. Q. Xu and J. R. Lombardi, *J. Phys. Chem. C*, 2008, 112, 20095–20098.
2. X. Wang, W. Shi, Z. Jin, W. Huang, J. Lin, G. Ma, S. Li and L. Guo, *Angew. Chem., Int. Ed.*, 2017, 56, 9851-9855.
3. X. Q. Fu, F. L. Bei, X. Wang, X. J. Yang and L. D. Lu, *J. Raman Spectrosc.*, 2009, 40, 1290–1295.
4. Y. Wang, H. Hu, S. Jing, Y. Wang, Z. Sun, B. Zhao, C. Zhao and J. R. Lombardi, *Anal. Sci.*, 2007, 23, 787–791.
5. S. Cong, Y. Yuan, Z. Chen, J. Hou, M. Yang, Y. Su, Y. Zhang, L. Li, Q. Li, F. Geng and Z. Zhao, *Nat. Commun.*, 2015, 6, 7800.
6. Q. Zhao, G. Liu, H. Zhang, Y. Li and W. Cai, *Adv. Mater. Interfaces*, 2018, 5, 1700709.